Sand ripple volume generator for underwater acoustic models, a cellular automaton Monte-Carlo approach.

P. Staelens[(1)], Y. Dupont[(2)], J.-P. Henriet[(3)]

1. dotOcean N.V., Brugge, B – peter@dotocean.eu
2. Belgian Navy, Brussels, B – yves.dupont@mil.be
3. Renard Centre of Marine Geology Ghent University, Gent, B – jeanpierre.henriet@ugent.be

Abstract

Cellular automata have been successfully used to model the sand dynamics of aeolian dunes and ripples. The cellular automata Monte-Carlo model proposed in this paper expands the capabilities of cellular automata models to under water ripple formation introducing not a two dimensional matrix but two three dimensional volumes, being a sand volume and a water volume. The proposed model has the capability to generate optimal environmental data to input in other mathematical models in need of environmental data. The following enhancements were implemented: optional abstraction levels of the hydrodynamic behavior, morphological formation of underwater ripples under unilateral currents in any direction as well as morphological formation of underwater ripples under wave current interaction, grain size distribution of the sand in every time step in the entire volume and compaction distribution in every time step in the entire sediment volume. The proposed cellular automata model is a closed toroidal system. The toroidal approach of the model enables to build up infinite rippled surfaces by using the generated sediment volumes as tiles; this solves boundary problems in for example acoustic models. Using the fractal properties of the sand ripples, infinite surfaces containing rippled dunes can be generated.

1. INTRODUCTION

A sandy seafloor is covered with bedforms, the bedform dynamics themselves sorting and compacting the sediment (Soulsby 1997). Understanding the complex non-random sediment dynamics in general and the interaction with sea mines is essential to understand the resulting acoustic response of sediment and semi buried or buried mines. Bedforms can be observed in any sandy environment where the shear stress caused by a current over a sand bed exceeds a certain threshold (Soulsby 1997). Once the threshold is exceeded, the granular medium reorganizes itself from a rough, relatively flat morphology into a ripple pattern. Sand ripples and dunes can be seen as self organizing patterns with a fractal character (Tian-De, Qing-Song et al. 2001). The fractal property will prove to be useful in the acoustic models. Ripples and dunes may be generated by a sub aqueous current or by the wind (aeolian ripples). Aeolian generated patterns have been described and modeled by Nishimori and Ouchi (Nishimori and Ouchi 1993), Anderson and Bunas (Anderson and Bunas 1993), Landry and Werner (Landry and Werner 1994), Yizhaq et al. (Yizhaq, Balmforth et al. 2004) gives a brief overview of some existing aeolian models and model approaches. Many expansions on these models have been made in the recent decade. Soulsby (Soulsby 1997) explains the sub aqueous transport mechanisms, but does not propose any model. The aeolian sediment transport processes and formulae as described (Anderson and Bunas 1993; Nishimori and Ouchi 1993; Landry and Werner 1994; Tian-De, Qing-Song et al. 2001; Zhang and Miao 2003; Yizhaq, Balmforth et al. 2004) do not apply in sub aqueous environments, but the resulting shapes and some patterns are similar. Therefore first existing aeolian models were evaluated and found to be inapplicable in underwater acoustic models. The models proved to be inapplicable in underwater acoustics because they were not designed to generate the parameters such as grain size distribution and compactions. Upgrading the models to an applicable level for underwater acoustics appeared to be impossible. Nevertheless a lot can be learned from the methodological approach some of the authors

have. In this paper the toroidal cellular automaton approach will be used. On the application level, to prevent algorithmic implementation effects in the data, a Monte-Carlo method has been used to trigger the automata. The goal is not to regenerate the sediment volume using exact rules corresponding fully with nature; the goal of this model is to generate artificial sediment with a correct distribution of required properties and to avoid synthetically looking surfaces generating synthetic results in mathematical models where the generated volumes are used as input. The distribution at a micro level often is random; on higher levels the distribution often appears to have unique but recognizable patterns. The properties covered in this paper will be: topography, grain size distribution, compaction and acoustic impedances.

2. METHOD

The cellular automata technique used in this paper is based upon the behavioural description of one single sand grain, called a cellular automaton, in a cellular automata system. The 3D cellular automata matrix used in the presented simulations typically includes a layered set of 5.000.000 automata, all having the same rules, but with different attributes such as weight and dimensions. As previously stated, the automata are triggered using a Monte-Carlo method and only sand grains exposed to fluid flow can be triggered. This generally reduces the amount of activated automata per time step, in the presented simulations, to about 0.1% or 5.000. The model as such does not contain every sand grain available in a real life system, but reduces the behaviour of a predefined zone or bin of sand to one single sand grain called the cellular automaton. The bin dimensions are defined by the user.

Four transport mechanisms are active in a sub aqueous sand dynamic system. The transport mechanisms are implemented on the cellular automata, they are; avalanche, roll, saltation and creep. In this model a combination of roll and saltation is the driving mechanism of sub aqueous sediment transport; a grain rolls or hops up the ripple following the least energy-consuming path to the crest where it may avalanche until it settles down in the current shadow. If a pile of grains exceeds a certain stability angle, the pile will fail and grains will avalanche until a specific stability angle has been restored. The stability angle of sand in a non-energetic environment is about 32°-37° (Soulsby 1997). Saltation is the most energy consuming way of transport. Saltation means that grains are ejected from the sand bed, float in the water column and splash down downstream. Saltation is thought to be the driving mechanism for aeolian ripple formation (Anderson and Bunas 1993; Nishimori and Ouchi 1993; Landry and Werner 1994; Tian-De, Qing-Song et al. 2001; Yizhaq, Balmforth et al. 2004). When fixed time step increments are introduced, a grey region between roll and saltation emerges. A single grain may have contact several times with the seabed in a single time step. In order to reduce the complexity of the model and allow the usage of fixed time step intervals, saltation and roll are approached as being one mechanism. All grain movements influenced by more than one small scale feature of the sand bed during one discrete time increment (hopping) follow the roll equations. Since most of the bedload transport happens near to the seabed, most of the saltation movements can be described as 'hopping' in the proposed model. Other forms of saltation can be implemented, but will be ignored in this implementation. The fourth mechanism is the creep mechanism; some grains have minimal exposure to the current and destabilize, they however do not receive enough energy to roll up the ripple. These grains will modify their position on the ripple slope, they might move to an adjacent bin. This mechanism can be seen as the settling of the sand grain in a nearby optimal position and makes the surface smoother and more realistic looking.

2.1. Two dimensional implementation

Starting with a simplified 2D approach of ripple formation, the model adopts the following sedimentological rules. Figure 9 shows a ripple and a coordinate system. The current flows in the positive X direction. The transport mechanisms can be subdivided in two groups: energy consuming mechanisms such as saltation, roll and creep and energy producing mechanisms as avalanching and sometimes creep. The system will receive energy from the avalanching when a slope gradient in the system exceeds the stability angle,

that angle is called α. The energy consuming mechanisms also have some stability angles. The angle β defines the maximum slope of the stoss side of the ripple. The current shadow is defined as h_x-h_{x-1}< 0. Where h is the topographic height of the considered bin, x and x-1, and the direction of the main current is along the positive X axis.

Consider now one single grain, with a diameter gd. An increasing force is imposed on it, forcing it to move or roll. The grain will have the potential to move once the implied force is higher than the friction force keeping the grain on its position. The model will translate the exerted force to energy. Per bin, per discrete unit of time a grain can spend a maximum accumulated amount of energy: Ex. Exposed grains and grains positioned on a slope exceeding the stability angle β will be transported over a distance s, following equation 1

$$s = \sum \Delta s \qquad (1)$$

With every discrete space step Δs defined as:

$$\Delta s = \sqrt{\Delta x^2 + (\Delta h + gd)^2} \quad (1)$$

The stoss side stability angle or β-function is not yet determined, β is set to an acceptable constant 7°, but is supposed to be related to the horizontal component of the water velocity vector on the sea floor, grain mass and smallest current impact surface of a grain. A similar approach can be made for the β_2-function related to vortices (Figure 1).

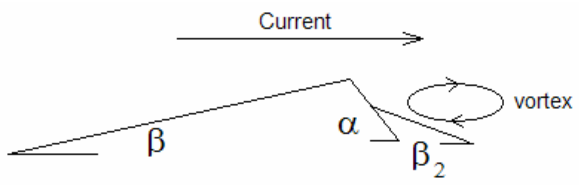

Figure 1. Stability angle schematics

A moving grain will spend an amount of energy per discrete space step.

$$E = \sum \Delta e \qquad (2)$$

Where Δe is defined as the energy used in a movement between two adjacent bins. The grain will stop rolling as soon as the grain enters a bin where E ≥ E_x.

The last rule of the roll movement defines that all grains in a current shadow, h_x-h_{x-1} < 0, will not move at all, the hydrodynamics matrix can provide that information. The α-function, or avalanche function, is set to a constant: 32°. The summary of formulae for the energy consumption in roll, with a current in the positive X direction, is given in the equation set 3.

$$\begin{cases} E = \sum \Delta e \\ E \le E_x \\ E_x = 0 \Leftrightarrow h_x - h_{x-1} < 0 \\ E_x = 0 \Leftrightarrow \begin{cases} h_x - h_{x-1} < h_{x+1} - h_x \\ \dfrac{h_x - h_{x+1}}{\Delta x} < \beta \end{cases} \end{cases} \qquad (3)$$

The discrete energy consumption Δe is defined as the sum of the energy used to overcome the friction (Efriction) and the energy used to lift up the grain (Egravity). Efriction is a function of mass and travelling distance, while Egravity is a function of mass and the difference in height between two adjacent bins x and x+1:

$$\Delta e = E_{friction}(m, \Delta s) + E_{gravity}(m, \Delta h) \qquad (4)$$

The grain movement rules for roll and bed load saltation are:

$$\begin{cases} h_x = h_x - gd \\ h_{x+1} = h_{x+1} + gd \end{cases} \Leftrightarrow \quad \Delta e > 0 \qquad (5)$$

And the grain movement rules for the avalanche:

$$\begin{cases} h_x = h_x - gd \\ h_{x+/-1} = h_{x+/-1} + gd \end{cases} \Leftrightarrow \quad \frac{h_x - h_{x+/-1}}{\Delta x} > \alpha \qquad (6)$$

Implementing this simple set of rules will generate a 2D section of a ripple taken parallel to the current. The avalanche mechanism is simplified, but demonstrates well the idea.

2.2. Three dimensional implementation

Imagine a number of 2D systems are set parallel to the flow current in a three dimensional matrix. Using the above rules, ripple shapes will appear in the matrix but no ripple pattern, all grains will move along the X axis. A ripple pattern is formed when a communication between each 2D ripple shape is possible. Here Δs, equation 2, as distance will be expanded to equation 7:

$$\Delta s = \sqrt{\Delta x^2 + \Delta y^2 + (\Delta h + gd)^2} \qquad (7)$$

As described in the sedimentation rules, a grain will follow the least energy consuming path, as a result in the roll movement there will be three options to roll to instead of one. The 3D expansion of the 2D rules for roll is given in equation 8 (assuming that roll is possible):

$$\Delta e_{optimal} = \min \begin{bmatrix} \Delta e_{x,y \to x+1,y-1} \\ \Delta e_{x,y \to x+1,y} \\ \Delta e_{x,y \to x+1,y+1} \end{bmatrix} \quad (8)$$

Avalanching will be similarly expanded, instead of two avalanche directions there will now be eight directions of avalanche (diagonals are included; most of the implementation applies calculations in an 8-cell Moore neighbourhood). The result of these expansions will be a 3D ripple like pattern (Figure 4, Figure 6, Figure 9). Avoiding undesired effects related to the discretisation can be done using the creep method or the implementation of a low pass filter along the Y axis. The stability angle γ for destabilized creeping grains will be related to the energy lost in friction and will be along the Y axis. This mechanism is of high importance to expand the 2D model to a 3D model since it will act as a low-pass filter along the Y axis. Filters along the Y axis are often implemented in the code implementation of the described aeolian ripple models. Implementing filters gives optimal topographic results but reduces the model to a topographic model. Since we aim to derive some basic parameters such as compaction and grain size distribution, filters cannot be implemented in this application. The creep method allows a grain to move to one adjacent bin in the Von Neumann neighbourhood if the grain is exposed to the current. Creep movement will not take energy out of the system. In order to have creep, a grain must have sufficient exposure to the flow current, hcreep is a Boolean derived from the formula below and defines whether a grain can move or not (reduced Moore neighbourhood).

$$h_{creep} = \min \begin{bmatrix} h_{x-1,y-1} \\ h_{x-1,y} \\ h_{x-1,y+1} \end{bmatrix} \leq h_{x,y} - gd - \gamma \Delta s \quad (9)$$

The creeping grain can be exposed but must also be able to settle, this time, in a reduced Von Neumann neighbourhood. The Boolean hoptimalset defines whether the grain can settle.

$$h_{optimalset} = \min \begin{bmatrix} h_{x,y-1} \\ h_{x,y+1} \\ h_{x+1,y} \end{bmatrix} \leq h_{x,y} - gd - \gamma \Delta s \quad (10)$$

If both hcreep and hoptimalset are true, a creep motion will be invoked and the grain will move to an adjacent cell with minimum height.

2.3 The hydrodynamic volume

The hydrodynamic volume generator is separated from the sedimentological model and is activated after each run or time step of the sedimentological model. In the presented data, the hydrodynamic volume generator applies a simple set of rules. Infinite complexity of the hydrodynamic volume generator is not possible without adapting some of the rules applied in the sedimentological model. The decision of the cellular automaton or sand grain to follow the lowest energy consuming path is equal to what the water particles would do. Implementing similar rules in the hydrodynamic module would accelerate the particles. One has to make the choice on where to apply what set of rules. The hydrodynamic model used in the presented simulations is one that generates a current shadow behind the ripple crest (Figure 2).

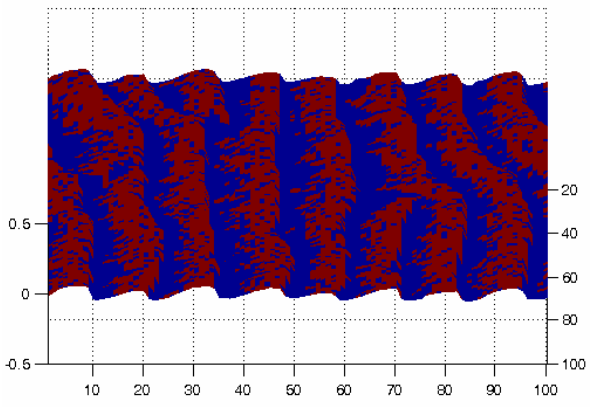

Figure 2. In red are the grains in motion, blue shows the grains in the current shadow.

The hydrodynamic model starts with horizontally slicing the water volume and implements a speed vector to all slices that encounter no obstruction. When passing an obstruction or ripple crest the

bins behind the obstruction are set to zero over a predefined distance. Every hydrodynamic slice drags the underlying slice with a predefined delay in the space domain. Depending on the height of the crest, the topography behind the crest, the number of horizontal hydrodynamic slices and the viscosity rules set, the water flow will pick up speed again closer or further behind the crest.

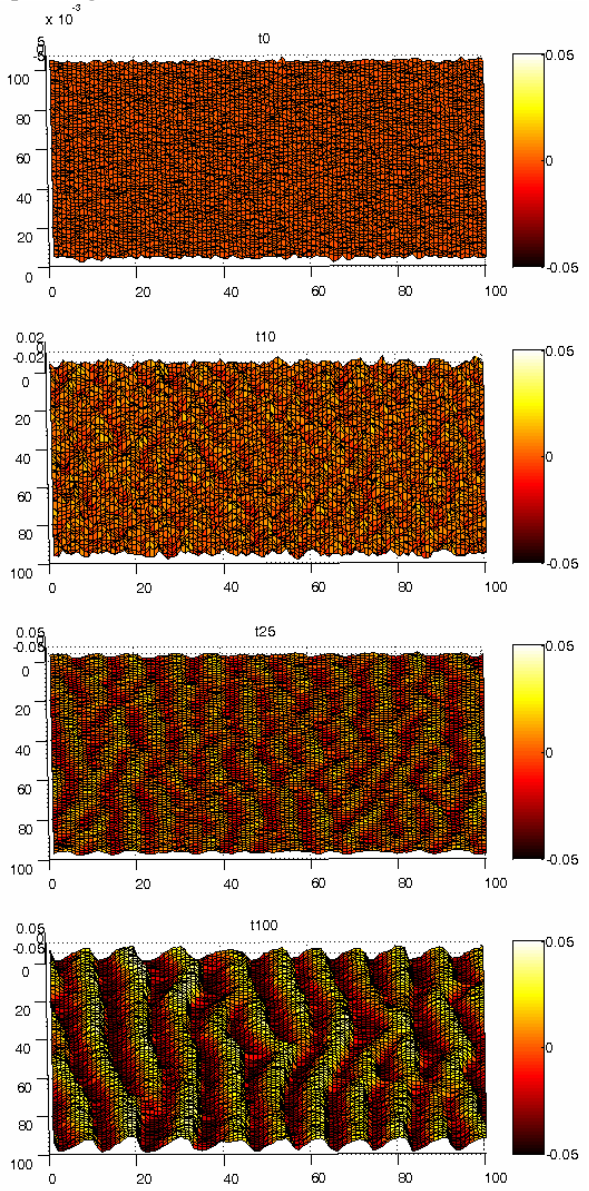

Figure 3. Topographic evolution from a rough surface to a rippled surface is demonstrated. Initial condition t0 is the top figure followed by time steps t10, t25 and t100.

3. RESULTS AND APPLICATIONS

The cellular automaton rules set and explained are the basic rules for a simple model and are subject to modification. Extra restrictions or open up restrictions is possible. The proposed rules compensate largely for small scale hydrodynamic variations but not for vortices.

3.1 Evolution of a ripple field

Figure 3 displays the evolution in 4 time steps of a rough flat sand surface to a ripple field. This example has been generated using a unilateral current. Simulating wave interaction using the proposed cellular automata rules is possible.

3.2 Acoustic impedance distribution

The generated results appear to be sufficient for acoustic modelling (Staelens (2009)). Next to topography, acousticians are also interested in acoustic impedances. The acoustic impedance of a sediment is a function of the sound speed trough the sediment and the density of the sediment. Densely packed sand has higher acoustic impedance than loosely packed sand. A complex mechanism as sand ripple evolution and migration generates a sorted sediment with a potential of very strong impedance changes. A simulation containing a compaction module generates Figure 4, the surface distribution of acoustic impedances in a ripple field.

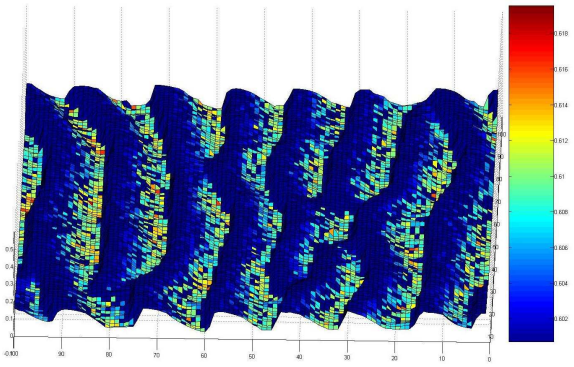

Figure 4. Generated acoustic impedance distribution on the surface of a ripple field, generated from a compaction module implemented on the sand ripple generator (dark blue is lower impedant)

3.3 Acoustic ray tracing

Another acoustic modelling application is ray tracing and formation of shadows. Acoustic ray bending in the simplest form is function of the sound velocity variations in the water column and the opening angle of the sonar. The formation of shadows depends upon the vertical sound velocity profile, the sonar opening angle and the seafloor (Figure 5).

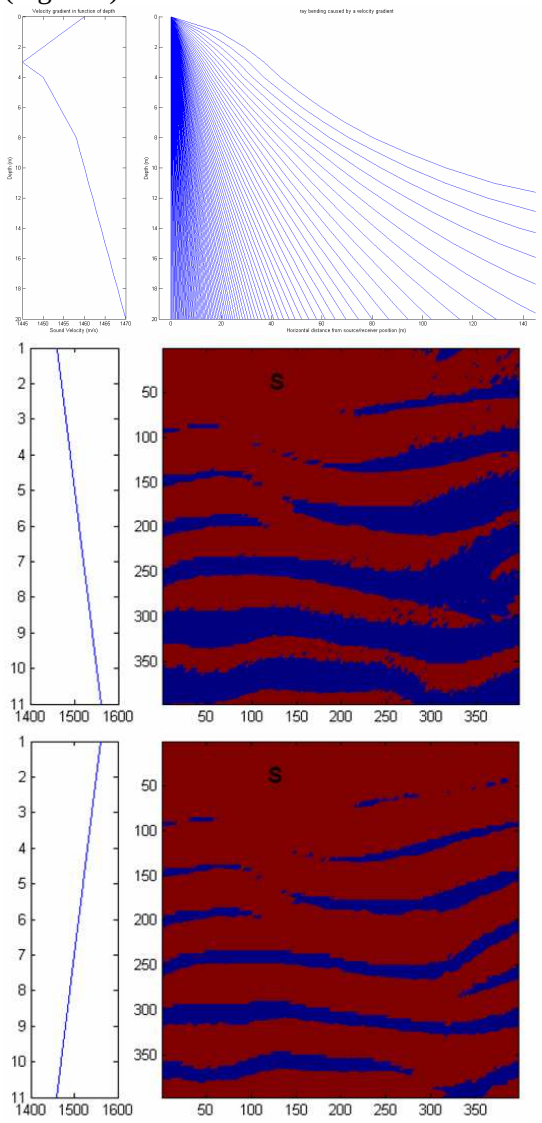

Figure 5. All figures have on the left the sound velocity variation in function of depth. The top figure shows the principle of ray tracing in function of the opening angle of the sonar. The centre and bottom figure display the effect on shadowing based on a sound velocity profile, S is the position of the acoustic transducer.

3.4 Generating an infinite surface

Tiling up the artificial environment is possible (Figure 6) and allows the generation of continuous infinite surfaces without holes or gaps. The neighboring tiles can be tiles from the same time step or, since changes in between time steps are relatively small, can be from different but close time steps. The last feature described allows the generation of ripple patches. Fractal properties of dunes can be used to generate rippled dunes (Figure 9)

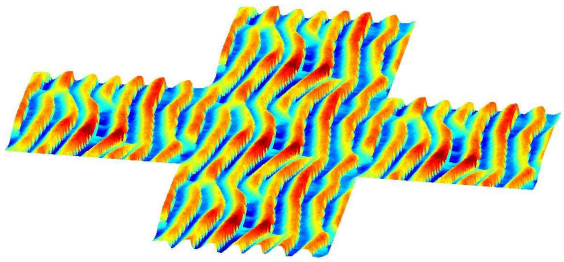

Figure 6. Ripple tiles are being used to generate an infinite surface without boundary gaps

3.5 Grain size distribution

A vertical section through the sediment volume displays a sorting of the sediment (Figure 7). Finer grains appear to concentrate in the ripples features. Figure 8 shows the grain size distribution on the surface of the ripple. This observation is to be verified.

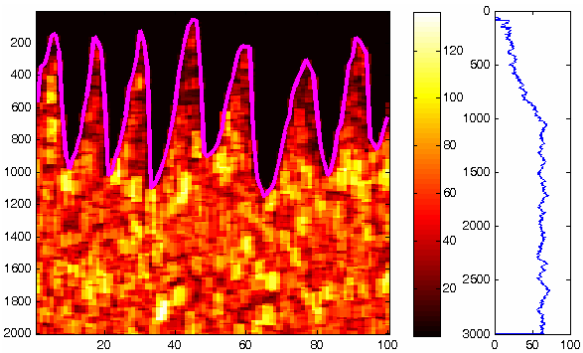

Figure 7. grain size distribution after an 8-cell Moore neighborhood average filter in a vertical section of the generated sediment volume (left) and the average grain size evolution in function of depth over the profile (right)

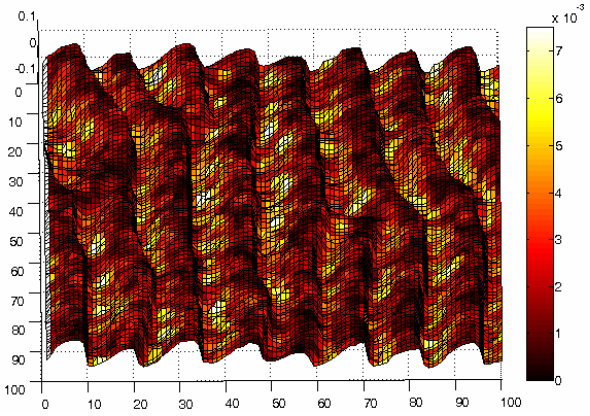

Figure 8. Grain size distribution on the surface after an 8-cell Moore neighborhood average filter. In the ripple through the larger or heavier particles appear to concentrate.

4. CONCLUSIONS

Modeling sand dynamics using cellular automata in combination with a Monte Carlo method implementation appears to deliver high quality data for mathematical models in need of unbiased sediment input data. Correct implementation of the methodology allows the generation of additional parameters needed in for example underwater acoustic models. The major advantage of using digital generated sediment volumes instead of, for example multibeam echosounder generated maps, in underwater acoustic models is that the digital sediment volume is free of interpretation and allows as such validation of for example backscatter interpretations and fundamental research on sonar imaging technology. Applying additional modules on the cellular automata model allows the generation of new parameters. The demonstrated grain size distribution effects need to be validated on the field or in lab conditions. This validation will probably add additional rules to the cellular automata but will increase reliability of the model.

5. ACKNOWLEDGMENT

This research was funded by the Belgian Navy and supported by Ghent University.

6. REFERENCES

Anderson, R. S. and K. L. Bunas 1993. Grain-Size Segregation and Stratigraphy in Aeolian Ripples Modeled with a Cellular-Automaton. Nature 365(6448): 740-743.

Nishimori, H. and N. Ouchi 1993. Formation of Ripple Patterns and Dunes by Wind-Blown Sand. Physical Review Letters 71(17): 2841-2841.

Landry, W. and B. T. Werner 1994. Computer-Simulations of Self-Organized Wind Ripple Patterns. Physica D 77(1-3): 238-260.

Soulsby, D.H. (1997). Dynamics of marine sands. A manual for practical applications, Thomas Telford Publications, London, England, 249 p.

Staelens, P.J.M. 2009. Defining and modeling the limits of high-resolution underwater acoustic imaging. Ph.D. thesis, UGent. 178 pp.

Tian-De, M., M. Qing-Song, et al. 2001. Computer simulation of aeolian sand ripples and dunes. Physics Letters A 288(1): 16-22.

Yizhaq H., Balmforth N.J., Provenzale A. (2004). Blown by wind: nonlinear dynamics of aeolian sand ripples. Physica D 195: 207-228.

Zhang, Q. H. and T. D. Miao 2003. Aeolian sand ripples around plants. Physical Review E 67(5).

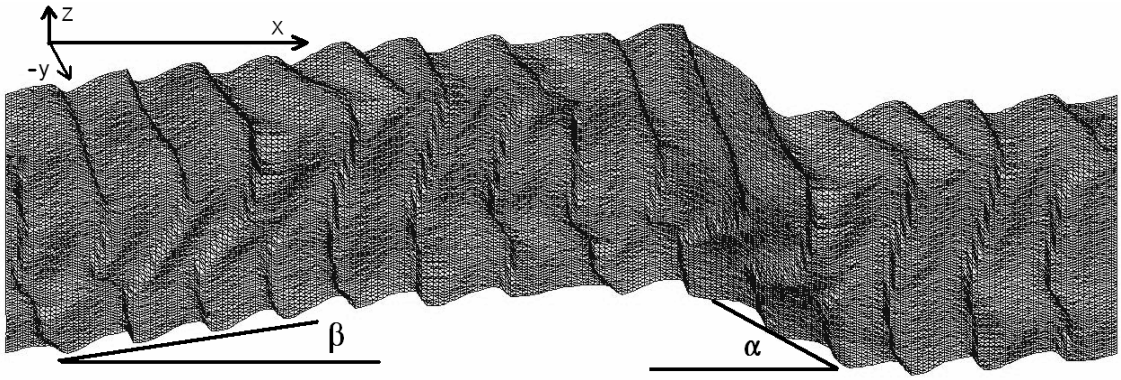

Figure 9. The coordinate system used during the simulations displayed on a fractal implementation of the generated ripple topography.